VCU

VIRGINIA COMMONWEALTH UNIVERSITY

Virginia Commonwealth University
VCU Scholars Compass

Physics Publications

Dept. of Physics

2008

Interaction of gas molecules with Ti-benzene complexes

G. Chen
Virginia Commonwealth University

P. Jena
Virginia Commonwealth University, pjena@vcu.edu

Y. Kawazoe
Tohoku University

Follow this and additional works at: http://scholarscompass.vcu.edu/phys_pubs

Part of the Physics Commons

Downloaded from

Interaction of gas molecules with Ti-benzene complexes

G. Chen,[1] P. Jena,[1] and Y. Kawazoe[2]

[1]*Department of Physics, Virginia Commonwealth University, Richmond, Virginia 23284, USA*
[2]*Institute for Materials Research, Tohoku University, Aoba-ku, Sendai 980-8577, Japan*

Using first-principles calculations based on gradient corrected density functional theory, we have studied the interaction of NH_3, H_2, and O_2 with Ti-benzene complexes [$Ti(Bz)_2$ and $Ti_2(Bz)_2$]. The energy barriers as the gas molecules approach the Ti-benzene complexes as well as the geometries of the ground state of these interacting complexes were obtained by starting with several initial configurations. While NH_3 and H_2 were found to physisorb on the $Ti(Bz)_2$ complex, the O_2 reacts with it strongly leading to dissociative chemisorption of the oxygen molecule. In contrast all the gas molecules react with the $Ti_2(Bz)_2$ complex. These studies indicate that the reaction of certain, but not all, gas molecules can be used to probe the equilibrium geometries of organometallic complexes. Under special conditions, such as high pressure, the Ti atom intercalated between benzene molecules in $Ti(Bz)_2$ and the $Ti_2(Bz)_2$ complexes could store hydrogen in chemisorbed states. The results are compared to available experimental data. © *2008 American Institute of Physics.*
[DOI: 10.1063/1.2969108]

I. INTRODUCTION

The interaction between metal atoms and organic molecules has been a topic of great interest in organometallic chemistry for a long time. However, a fundamental understanding of the structure of these systems and, in particular, how and where the metal atoms bind to the organic molecules has been difficult to discern due to problems associated with solvents. The ability to make clusters of the organometallic complexes by varying both the number of metal atoms and organic molecules independently in the gas phase has made it possible to achieve this understanding. Many experiments[1–6] have been carried out in recent years that involve mass spectra, fragmentation channels, and electronic properties of transition and nontransition metal atoms interacting with different organic molecules. Since no experiments in the gas phase are able to directly describe the geometry of these complexes, indirect methods have often been employed. One such method is the study of the interaction of clusters with known gases and inferring geometries based on the reaction products. For example, Kaya and co-workers described a technique where transition metal-benzene complexes were reacted with NH_3. They found that among $M_x(Bz)_y$ complexes, where M is an early transition metal atom (Sc–V), those with $x=y$ reacted while those with $y=x+1$ did not. The authors suggested that these complexes have a sandwich structure, where the metal atoms are intercalated between the benzene molecules. For clusters with $x=y$, one metal atom is always exposed and hence can react, while for complexes with $y=x+1$, all the metal atoms are sandwiched between organic molecules and hence they are not exposed to the reactant molecules. The authors used CO and NH_3 as reacting gases. No theoretical studies have been carried out to study these reactions and confirm the experimental hypothesis. In addition, it is not clear if this suggestion is universal in the sense that it applies to all reagent gases or is it

specific to CO and NH_3? Pandey *et al.*[7] reported a comprehensive theoretical study of these complexes and confirmed the sandwich structure. However, no theoretical study has been reported on the interaction between the reagent gas molecules and the adsorbed metal atoms in these complexes.

In this paper, we provide the results of a theoretical study of the interaction of NH_3, H_2, and O_2 molecules adsorbed on $Ti(Bz)_2$ and $Ti_2(Bz)_2$ complexes. The metal-organic complexes describe two model systems—first, where one of the metal atoms is exposed, and second, where all the metals atoms are sandwiched between organic molecules. The reasons for selecting NH_3, H_2, and O_2 are as follows: (a) calculations on NH_3 will complement the experimental study; (b) H_2 molecules are small and steric hindrance may not be a major obstacle in allowing these molecules to react with metal atom sandwiched between the benzene molecules. In addition, several studies[8–12] have recently shown the promising ability of metal decorated polymers to store hydrogen. (c) Most metals exposed to air oxidize. Do the metal atoms oxidize when they are sandwiched between organic molecules? In the following a detailed study of the physical and chemical adsorption processes of NH_3, H_2, and O_2 on Ti-Bz complexes and the reaction paths between different states are presented. In addition to achieving a fundamental understanding of the interaction between the metal atoms and benzene, the results may shed light on their potential applications.

II. DETAILS OF CALCULATIONS

The calculations of binding energies and equilibrium structures were carried out using first-principles method based on the spin-polarized density functional theory (DFT),[13,14] as implemented in the Vienna *ab initio* simulation package (VASP).[15–19] We have employed the projector augmented-wave method.[17,18] The exchange-correlation con-

tribution to the potential is calculated using the generalized gradient approximation prescribed by Perdew–Wang (PW91).[20,21] The solution of the Kohn–Sham equations is performed by an efficient matrix diagonalization technique based on a sequential band-by-band residual minimization method.[16] A supercell with edge length of 18 Å is used in the calculations, which is large enough to eliminate the interaction between a complex and its periodic images. The charge density and the local potential are calculated using a $150 \times 150 \times 150$ mesh. The wave functions are expanded in a plane wave basis with an energy cutoff of 400.0 eV, which has been shown to be sufficient for Ti.[17–19] Only the Γ point in the supercell is used in the summation of the Brillouin zone. The optimization is stopped when the forces acting on each atom reach the force tolerance of 0.02 eV/Å.

We first discuss the accuracy of the DFT for treating Ti-benzene complexes since it has been pointed out by Rabilloud[22] that the ground state spin multiplicity of early transition metal-benzene complexes calculated using multireference configuration interaction (MRCI) calculation is at odds with those predicted by DFT.[7] For example, the spin multiplicity of VBz complex calculated by Pandey *et al.*[7] using DFT yielded a sextet state ground state, while that using MRCI[22] leads to a quartet state. Note that the energy difference between adjacent spin multiplicity states is close in energy and is sensitive not only to approximations in exchange and correlation potential but also to choice of basis sets. Kandalam *et al.*[23] showed that the ground state of the VBz complex using Lanl2dz basis set yields a spin quartet ground state, while that using a $6-311$ G** yields a spin doublet ground state, although both calculations were performed within the framework of DFT. The energy difference between the two spin states lies in the 0.3 eV energy range. However, this sextet state conflicts with the results of Yasuike *et al.*[6] Yasuike *et al.*[6] used a configuration-averaged self-consistent-field method which is similar in concept to that of the state-averaged multiconfiguration self-consistent-field (MCSCF) method of Rabilloud.[22] While both authors predicted a spin quartet ground state for VBz, the energy differences between the spin quartet and spin doublet states are found to be 0.44 eV by Rabilloud and 0.05 eV by Yasuike *et al.*[6] Using DFT and the projector augmented-wave method as implemented in the VASP code, we found the VBz ground state to have a spin doublet electronic configuration, which agrees with the Gaussian $6-311$ G** result of Kanadalam *et al.*[23] We also calculated the ground state spin multiplicity of TiBz complex using the method described above. Our computed spin multiplicity of 5 is in good agreement with the calculation of Yasuike *et al.*[6] who used a quantum chemical approach. For the Ti(Bz)$_2$ and Ti$_2$(Bz)$_2$ complexes studied in this paper, we calculated them to be singlet and quintet states, respectively.

To further confirm the accuracy of our method, we calculated the binding energies and structural parameters of TiH, TiO, TiN, and H$_2$Ti=NH molecules. The interatomic distances of Ti–H, Ti–O, and Ti–N in the diatomic molecules are calculated to be 1.75, 1.63, 1.59 Å, and the length of Ti–H, Ti–N in H$_2$Ti=NH molecule are calculated to be 1.76 and 1.68 Å, respectively. The datum is in good agreement

with the experimental Ti–O bond length of 1.62 Å.[24] The calculated Ti–H and Ti–N bond lengths in H$_2$Ti=NH molecule also agree well with those calculated using MCSCF method,[25] namely, 1.81 and 1.70 Å. The binding energies of TiH, TiO, and TiN molecules are calculated to be 2.62, 7.69, and 5.45 eV, which also agree well with the experimental values[24] of 2.12, 6.97, and 4.93 eV, respectively. These comparisons provide enough confidence in the accuracy of our computational technique. In addition, we should point out that while the binding energies and ground state spin multiplicites derived from various theoretical methods may differ, the equilibrium geometries are seldom sensitive to these choices. In this paper we are particularly interested in the structure of TiBz complexes as they react with gas molecules.

III. RESULTS AND DISCUSSIONS

The geometrical structures of Ti-benzene complexes with adsorbed gas molecules were obtained without imposing any symmetry constraint. For initial configurations we considered the molecules to bind to the Ti-Bz complexes in three possible ways: physisorption where the molecule is weakly bound; molecular chemisorptions where the molecular bonds are slightly stretched and binding is stronger than that in the physical adsorption state; and dissociative chemisorptions where the binding is the strongest and gas molecules dissociate and bind atomically. The reaction paths between different adsorption states were studied in detail. In Figs. 1, 3, and 5 we mark these configurations with symbols *P*, MC, and DC which represent, respectively, gas molecules bound in physisorbed state, molecular chemisorbed state and dissociative chemsorbed state. For each of these states, the molecules were initially allowed to approach the Ti-Bz complexes along the two different directions; the first one, denoted by symbol *V*, corresponds to the direction parallel to the C atom, while the second one, denoted by symbol *B*, corresponds to the direction parallel to the C–C bridge. These starting configurations are marked PB, PV, MCV, MCB, DCV, and DCB in Figs. 1, 3, and 5. For each of these starting configurations, we optimized the structures fully without symmetry constraint. In the following the results for each of the molecule interaction are discussed separately.

A. NH$_3$ adsorbed Ti-benzene complexes

The optimized geometrical configurations of NH$_3$ adsorbed on Ti(Bz)$_2$ and Ti$_2$(Bz)$_2$ complexes are shown in Figs. 1(a)–1(j), respectively. The binding energies, $\Delta E = E(M_xBz_y) + E(NH_3) - E(M_xBz_yNH_3)$, for each of the configurations are listed in Fig. 1. Note that positive binding energy means that the complex is bound while negative binding energy relates to unstable configuration. Energetically NH$_3$ prefers to bind to Ti(Bz)$_2$ in the physisorbed state (see the configurations marked PV and PB sates) with the geometry marked PV having marginally higher binding energy than that marked PB. The binding energy of the configuration marked PV is 60 meV, while that marked PB is 40 meV. The molecular chemical adsorption states MCV and MCB as well as the dissociative chemisorption adsorption states DCV
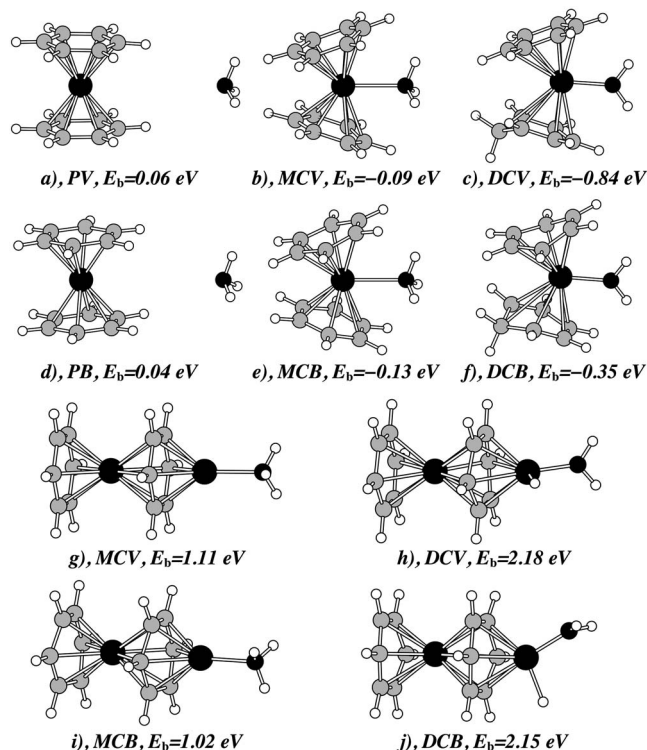
FIG. 1. The optimized geometries of NH_3 adsorbed on Ti-benzene complexes. The white, the gray, the big black, and the small black balls represent H, C, Ti, and N atoms, respectively. (a) and (d) are the physisorption states for $Ti(Bz)_2$; (b) and (e) are the molecular chemisorption states for $Ti(Bz)_2$; (c) and (f) are the dissociative chemisorption states for $Ti(Bz)_2$; (g) and (i) are the molecular chemical adsorption states for $Ti_2(Bz)_2$; and (h) and (j) are the dissociated chemical adsorption states for $Ti_2(Bz)_2$.
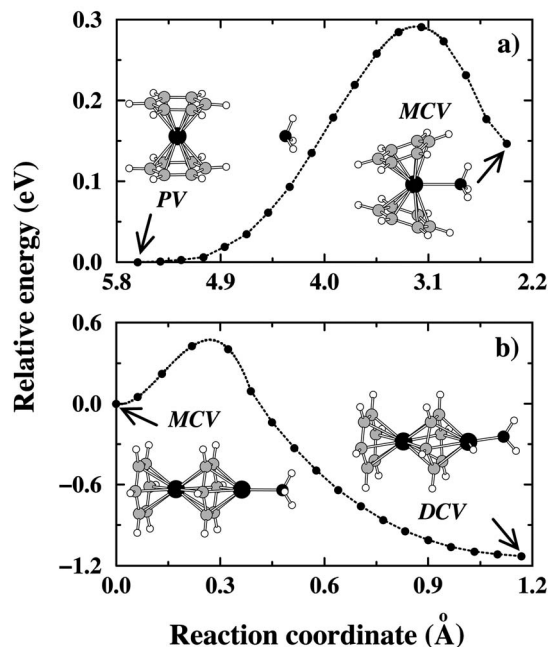

FIG. 2. Converged minimum energy paths calculated using the elastic band method. (a) The reaction path between the PV and MCV states for NH_3 adsorbed $Ti(Bz)_2$ complex. The total energy of PV state is used as the reference, and the interatomic distance between Ti and N atoms is used as the reaction coordinate; (b) the path between the MCV and DCV states for NH_3 adsorbed $Ti_2(Bz)_2$ complex. The total energy relative to that of MCV state is plotted, and the deviation of N atom from that of MCV state is plotted as the reaction coordinate.

and DCB of NH_3 have negative binding energies and hence are unstable. The interatomic distance between Ti and N in both PV and PB states is found to be ~ 5.62 Å, which is much longer than the sum of the atomic radii of N and Ti atoms (the atomic radii of Ti, N, and H atoms are 1.40, 0.65, and 0.25 Å).[26] This result is in agreement with experimental finding that NH_3 does not interact with Ti_nBz_{n+1} complexes.

For NH_3 interacting with $Ti_2(Bz)_2$, the situation is entirely different. Here both the molecularly chemisorbed and dissociatively chemisorbed states have positive binding energies. The binding energies of the molecular chemisorption states, MCV and MCB, are, respectively, 1.11 and 1.02 eV, while the binding energies of the dissociative chemisorbed states DCV and DCB are, respectively, 2.18 and 2.15 eV. The lowest energy configuration of NH_3 adsorbed on $Ti_2(Bz)_2$ is the DCV state and has a spin triplet electronic configuration. The DCB state has a multiplicity of 1 and lies 30 meV lower in binding energy than the DCV state. The interatomic distance between N and nearest Ti atom is 1.93 Å, and that between the top Ti atom and its nearest H atom is 1.75 Å. These distances are close to the sum of the atomic radii of corresponding atoms. The dissociative chemisorbed state NH_3 fragments into NH_2 and H with the H atom binding to the top Ti atom. The distance between the H and the N in NH_2 specie is 2.80 Å, which is much longer than that in NH_3 molecule of 1.02 Å.

The physisorption and the molecular chemisorption states of NH_3 on $Ti(Bz)_2$ complex have their binding ener-

gies differ only by about 0.16 eV. Thus by applying the pressure, it may be able to get NH_3 molecularly adsorb on $Ti(Bz)_2$. To study this possibility, calculations of the energy barrier between the molecular chemisorption and the physisorption states is needed. We calculated the energy barrier by using the elastic band method.[27–30] In Fig. 2(a), we show the converged results for the reaction path between PV and MCV states. The interatomic distance between the Ti atom and the N atom is selected as the reaction coordinate, and the total energy relative to that of PV state is used to measure the energy barrier. The energy barrier from the molecularly chemisorbed (MCV) state to the physisorbed (PV) state is only 0.14 eV, which could be easily overcome, and hence it may be difficult to trap the molecule in the MCV state. Thus in an experiment, once the molecular chemisorbed state is produced, a small perturbation such as heat could easily allow it to overcome the barrier to PV state, and hence it will be difficult to observe the binding of NH_3 to $Ti(Bz)_2$ complex. Figure 2(b) shows the converged minimum energy path between MCV and DCV states of NH_3 adsorbed on $Ti_2(Bz)_2$ complex. The $Ti_2(Bz)_2$ complex, due to the exposed Ti atom, reacts with the NH_3 molecule. The energy barrier between the above two states is calculated to be 0.43 eV. This small barrier can be overcome leading to the formation of the dissociative chemisorbed state as the final configuration. Experiment shows that Ti_nBz_n complexes are reactive, and this agrees with our theoretical result.

B. H_2 adsorbed Ti-benzene complexes

In Fig. 3, the optimized structures of H_2 adsorbed Ti-benzene complexes are presented. The PV and PB are the
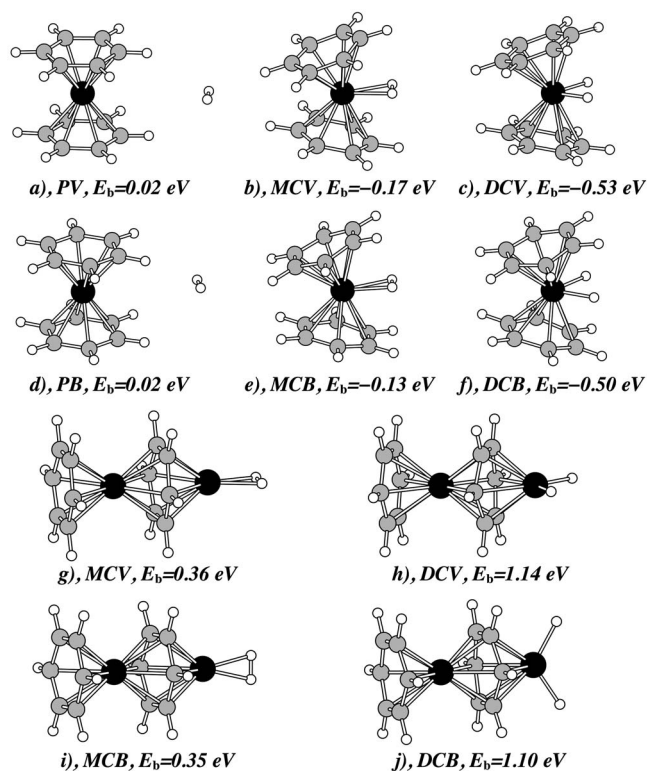
FIG. 3. The optimized adsorption configurations of H_2 adsorbed Ti-benzene complexes. The white, the gray, and the black balls represent H, C, and Ti atoms, respectively. (a) and (d) are the physisorption states for $Ti(Bz)_2$; (b) and (e) are the molecular chemical adsorption states for $Ti(Bz)_2$; (c) and (f) are the dissociative chemisorption states for $Ti(Bz)_2$; (g) and (i) are the molecular chemical adsorption states for $Ti_2(Bz)_2$; and (h) and (j) are the dissociative chemisorption states for $Ti_2(Bz)_2$.
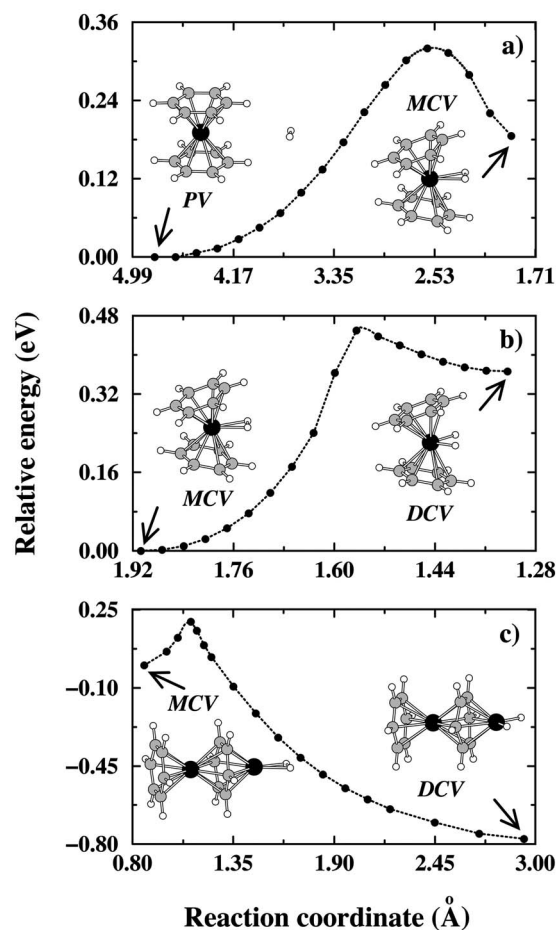

FIG. 4. Converged minimum energy paths calculated using the elastic band method. (a) The reaction path between the PV and MCV states for H_2 adsorbed $Ti(Bz)_2$ complex. The total energy of PV state is used as the reference, and the distance between Ti and the center of H–H bond is used as the reaction coordinate; (b) the path between the MCV and DCV states for H_2 adsorbed $Ti(Bz)_2$ complex. The total energy of MCV state is the reference, the H–H bond length is the reaction coordinate; (c) the reaction path between the MCV and DCV states for H_2 adsorbed $Ti_2(Bz)_2$ complex. The total energy relative to that of MCV state is plotted, and the H–H bond length is plotted as the reaction coordinate.

energetically preferred where H_2 is physisorbed on $Ti(Bz)_2$. Unlike the NH_3, the different configurations do not affect the binding energies of H_2 which are about 20 meV in physisorption states due to its small size. The states corresponding to molecular chemisorption or dissociative chemisorption are higher and the structure of $Ti(Bz)_2$ undergoes distortion. These chemisorption states have negative binding energies and hence are unstable. The interatomic distances between Ti atom and the H atom are 4.82 Å in the PV state and 4.52 Å in the PB state. The bond length of hydrogen molecule is 0.75 Å, while the bond length is elongated to $\sim$0.82 Å in MCV and MCB configurations, and to $\sim$2.10 Å in DCV and DCB configurations.

Analogous to that of NH_3, the equilibrium structure of H_2 interacting with $Ti_2(Bz)_2$ complex is very different from that of $Ti(Bz)_2$. There are no physisorbed states and the H_2 molecule is chemisorbed either molecularly or disssociatively with the later being lower energy configuration. The molecular chemical adsorption states (MCV and MCB states) have binding energies of $\sim$0.36 eV, while the binding energies of the dissociative chemisorption states (DCV and DCB states) are $\sim$1.12 eV. The ground state spin multiplicity for the DCV state is 3 and that for the DCB state is 1. The interatomic distances of the hydrogen molecule in the MCV and MCB states are about 0.86 Å, while that in the DCV and DCB states are $\sim$2.97 Å. The distances between

the top Ti atom to the H atoms are $\sim$1.95 Å in MCV and MCB configurations and $\sim$1.77 Å in DCV and DCB configurations.

We have calculated the energy barriers between the PV and MCV states and between the MCV and DCV states by applying the elastic band method. The results are shown in Fig. 4. In Fig. 4(a) the total energy relative to that of the PV state for H_2 adsorbed on $Ti(Bz)_2$ is plotted as a function of the reaction coordinate taken as the distance between the center of H–H bond and the Ti atom. The energy barrier for the MCV state to cross over to the PV state is 0.13 eV, while for transition of the PV state to the MCV state is 0.32 eV. These data show that under special experimental condition, the H_2 molecule could be stored in the chemisorbed state and can be released only after a small perturbation.

In Fig. 4(b), we present the reaction path between MCV and DCV states for H_2 adsorbed on the $Ti(Bz)_2$ complex. The total energy of MCV state is used as a reference. The distance between the two H atoms is again used as the reaction coordinate. The results clearly show that the energy bar-

riers for the transition from MCV to DCV and the reverse transition are 0.45 and 0.08 eV, respectively, which suggests that the hydrogen could be stored in dissociative chemical adsorption state under special conditions and the stored hydrogen could be released easily.

The converged reaction path between MCV and DCV states of H_2 adsorbed on $Ti_2(Bz)_2$ complex is shown in Fig. 4(c). The MCV state is used as the reference and the relative total energy is used to measure the energy evolution. The reaction coordinate is chosen as the distance between the two H atoms. The exposed Ti atom is reactive and incoming H_2 binds to the top Ti atom. As shown by our structural optimization study, the dissociative chemisorbed state of H_2 is the ground state, and the reaction process would release much heat due to the high binding energy. The incoming hydrogen molecule could bind in the molecular chemisorbed state and would transit to the final product of dissociative chemisorbed state by overcoming an ~ 0.20 eV energy barrier. The reverse process for releasing the hydrogen atoms adsorbed onto the Ti atom in DCV state has an ~ 1.0 eV energy barrier. The study of the reaction path shows that the H_2 could be easily bind dissociatively to the exposed Ti atom, but it will be hard to release it. It is possible that successive H_2 molecules to be bound to the exposed Ti atom with binding energies that will depend on of the number of attached molecules.

We have studied the dynamical properties of the above mentioned states by performing first-principles molecular dynamics (MD) simulation as implemented in VASP code. A microcanonical ensemble was used and the simulation lasted for 1 ps. We started the MD simulations at 500 K for the MCV and DCV states of H_2 adsorbed on $Ti(Bz)_2$, and for the MCV state of H_2 adsorbed on $Ti_2(Bz)_2$ (see the configurations shown as inserts in figure Fig. 4). The H_2 in molecular chemisorption state MCV on $Ti(Bz)_2$ flies away from the Ti atom and finally converges to the physisorption state PV during the simulation. The DCV state for H_2 adsorbed on $Ti(Bz)_2$ first evolves to the intermediate state MCV and then goes to the final product of the physisorption state PV. These results agree very well with our minimum energy path search which predicts that the energy barriers for the transitions from MCV to PV and DCV to MCV states for H_2 adsorbed on $Ti(Bz)_2$ complex are small and can be overcome at elevated temperatures. Similarly, the small energy barrier between the MCV and DCV states for H_2 adsorbed on $Ti_2(Bz)_2$ complex did not allow the MCV state to remain during the MD simulation. We also carried out MD simulation at 1500 K to further check the stability of the DCV state for H_2 adsorbed on $Ti_2(Bz)_2$ complex. Due to the high energy barrier found in our minimum energy path search, hydrogen atoms were trapped in the DCV state on the potential surface during the simulation. This suggests that it is hard to release hydrogen adsorbed in the dissociative chemisorption state DCV on a $Ti_2(Bz)_2$ complex.

The above results show that H_2 and NH_3 can both be used to shed light on the structure of T-Bz complexes. Ti_nBz_{n+1} complexes are not reactive while Ti_nBz_n complexes react. This establishes liner sandwich structures for these complexes.
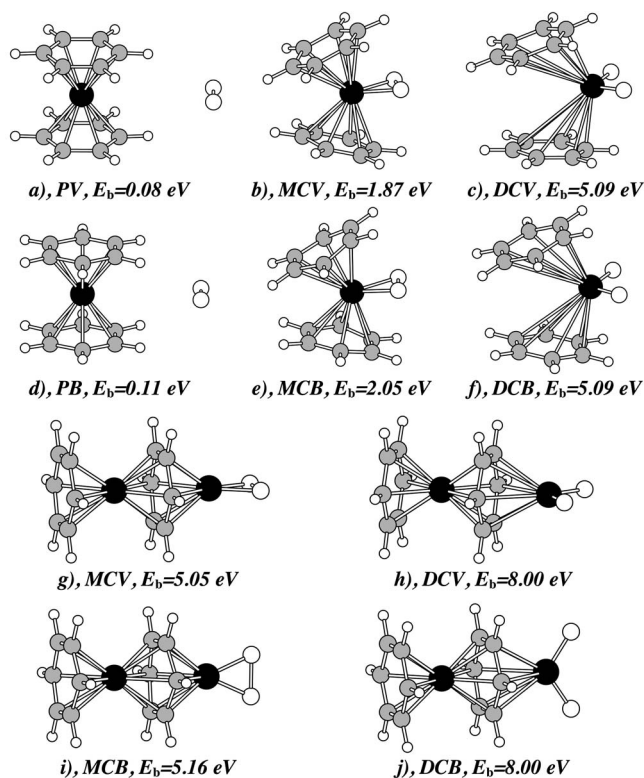

FIG. 5. The optimized geometries of O_2 adsorbed Ti-benzene complexes. The small white, the big white, the gray, and the black balls represent H, O, C, and Ti atoms, respectively. (a) and (d) are the physisorption states for $Ti(Bz)_2$; (b) and (e) are the molecular chemisorption states for $Ti(Bz)_2$; (c) and (f) are the dissociative chemisorption states for $Ti(Bz)_2$; (g) and (i) are the molecular chemisorption states for $Ti_2(Bz)_2$; and (h) and (j) are the dissociative chemisorption states for $Ti_2(Bz)_2$.

C. O_2 interacting Ti-benzene complexes

Finally, we have studied the reaction of O_2 molecules with Ti-Bz complexes. The results are given in Fig. 5. The O_2 molecule first physisorbs on the $Ti(Bz)_2$ complex. In this state both PV and PB configurations gain ~ 0.10 eV binding energies. The configuration PB is a little higher in binding energy than the PV configuration. The highest binding energy state, however, is the dissociative chemisorption state. The O_2 molecule dissociates and the O atoms bind to the Ti atom in $Ti(Bz)_2$ complex. The different configurations DCV and DCB have the same binding energies of 5.09 eV and the same spin singlet ground state. The molecular chemical adsorption states MCV and MCB for O_2 adsorbed $Ti(Bz)_2$ also have intermediate binding energies of 1.87 and 2.05 eV, respectively. The Ti–O distances are about 4.79, 1.92, and 1.68 Å in physisorption states, molecular chemisorbed states, and dissociative chemisorbed states, respectively. The O–O bond length is elongated from 1.26 Å in physisorbed state to 1.45 Å in molecular chemisorbed states, and finally reaches the 2.75 Å in dissociative chemisorption states. The length of O–O bond in the molecular chemisorbed state, namely, 1.45 Å, agrees very well with the peroxo bond of 1.45 Å in the TiO_2 complex.[31] The chemisorbed configuration of $Ti(Bz)_2$ complex experiences the largest distortion.

Figures 5(g)–5(j) show the structures of O_2 adsorbed onto the top Ti atom of $Ti_2(Bz)_2$ complex. The molecular

chemisorptions states MCV and MCB have higher binding energies than those of $Ti(Bz)_2$ complex, which are ~5.11 eV on average. The dissociative chemisorption states DCV and DCB have the largest binding energies of 8.00 eV. The interatomic distances between two O atoms are 1.49 and 2.79 Å for the molecular chemisorption state and the dissociative chemisorption states, respectively. The ground state spin multiplicities of the DCV and DCB states are singlet.

The best O_2 adsorption state on Ti-benzene complex is the dissociated chemisorbed state. To understand the oxidation process of Ti-benzene complex, we have performed detailed calculations using the elastic band method of the minimum energy paths between the PB and MCB states and the MCB and DCB states for O_2 adsorbed $Ti(Bz)_2$ complex and between the MCB and DCB states for O_2 adsorbed $Ti_2(Bz)_2$ complex. The total energy was found to decrease smoothly starting from the PB state toward the MCB state for O_2 on $Ti(Bz)_2$. However, the converged results did not show any energy barrier. We therefore carefully double checked the PB state for O_2 on $Ti(Bz)_2$ and confirmed that O_2 could exist in the physisorbed state. While a dense image elastic band calculation could be used to calculate the barrier, it is computer intensive. Therefore, we estimated the barrier by interpolating 31 points between the PB and MCB states on potential surface and calculating the total energy of each image while keeping the position of the atoms fixed. The energy barrier is estimated to be only 0.06 eV for transition from the PB state to the MCB state. Since the interpolation method could overestimate the barrier, the real energy barrier could be very small, and the physisorbed state of the O_2 molecule would evolve to the chemisorbed state almost spontaneously.

In Fig. 6(a) we plot the converged results based on the elastic band method between the MCB and DCB states for O_2 adsorbed on $Ti(Bz)_2$ complex. The total energy of MCB state is shifted to zero, and the relative energy is plotted as a function of the reaction coordinate which is the interatomic distance between two O atoms. The energy barrier is about 0.31 eV from the MCB state to the DCB state. So, a small perturbation could drive the molecularly chemisorbed O_2 molecule to dissociate into two separate oxygen atoms and bind to the Ti atom directly. The binding energies of the PB and DCB states are 0.11 and 5.09 eV, respectively. So, much heat would be released during the reaction.

For adsorption of O_2 on the $Ti_2(Bz)_2$ complex, our calculation again shows that there is no physisorbed state. The incoming O_2 could be attached to the top Ti atom and release more than 5 eV energy. Figure 6(b) presents the minimum energy path obtained by elastic band method for the evolution from the molecular chemisorption state MCB to the dissociative chemisorbed state DCB for O_2 adsorbed on $Ti_2(Bz)_2$ complex. The total energy relative to that of the MCB state is plotted. The reaction coordinate is the interatomic distance between two O atoms. One can see from the figure that the energy barrier is about 0.31 eV for the MCB state transitioning to the DCB state. Therefore, once the O_2 molecule is added to the $Ti_2(Bz)_2$ complex, it would dissociate fast under a small perturbation. It is likely that when the incoming O_2 molecule goes into the molecularly chemisorbed state, the heat released in the process would cause the
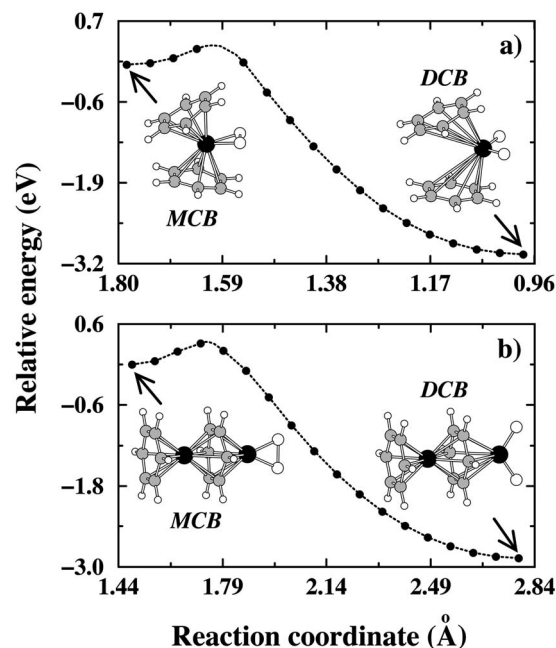

FIG. 6. Converged minimum energy paths calculated using the elastic band method. (a) The reaction path between the MCB and DCB states for O_2 adsorbed $Ti(Bz)_2$ complex. The total energy of MCB state is used as the reference, and the O–O bond length is used as the reaction coordinate; (b) the path between the MCB and DCB states for O_2 adsorbed $Ti_2(Bz)_2$ complex. The total energy relative to that of MCB state is plotted, and the O–O bond length is plotted as the reaction coordinate.

oxygen molecule to dissociate. The whole reaction would release about 8 eV energy as the incoming free oxygen molecule dissociates chemisorbs.

D. Electronic structure

In Fig. 7(a), we plot the total density of states (DOS) of $Ti(Bz)_2$. The DOSs for the NH_3, H_2, and O_2 adsorbed on $Ti(Bz)_2$ complexes corresponding to the highest binding energy structures are plotted in Figs. 7(b)–7(d), respectively. Similarly the DOS of $Ti_2(Bz)_2$ and those with NH_3, H_2, and O_2 adsorbed $Ti_2(Bz)_2$ complexes are shown in Figs. 7(e)–7(h), respectively. The dotted lines mark the *Fermi* energies.

The band gap between the highest occupied molecular orbital (HOMO) and the lowest unoccupied molecular orbital (LUMO) is 0.94 eV for the bare $Ti(Bz)_2$ complex. The $Ti_2(Bz)_2$ complex due to the top Ti atom has zero band gap, which suggests that it should be more reactive. The NH_3 and H_2 do not chemisorb on $Ti(Bz)_2$, however, they do react with the top Ti atom in $Ti_2(Bz)_2$. For the weak van der Waals interaction, physisorption of NH_3 and H_2 on $Ti(Bz)_2$ does not alter its DOS much and the band gaps of NH_3 and H_2 adsorbed on $Ti(Bz)_2$ complexes are 0.95 and 0.94 eV, respectively. The highest binding energy state for O_2 adsorbed $Ti(Bz)_2$ is the dissociative chemisorbed state. The binding of oxygen to the titanium significantly affects the electronic properties of $Ti(Bz)_2$. The band gap between HOMO and LUMO is enlarged to 2.0 eV. We have checked the band energies of the LUMO bands of freestanding NH_3, H_2, and O_2 molecules, which are −0.82, −0.01, and −4.96 eV, re-
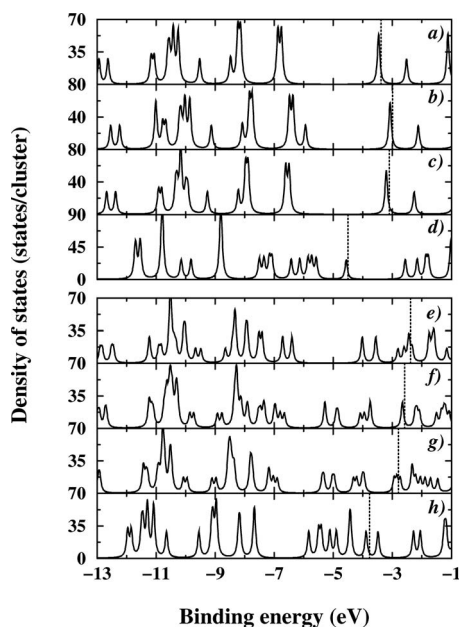
FIG. 7. DOS of (a) Ti(Bz)$_2$ complex and those [(b)–(d)] corresponding to the highest energy configurations of NH$_3$, H$_2$, and O$_2$ molecules adsorbed Ti(Bz)$_2$ DOS of (e) Ti$_2$(Bz)$_2$ complex and those [(f)–(h)] corresponding to the highest binding energy configurations of NH$_3$, H$_2$, and O$_2$ molecules adsorbed Ti$_2$(Bz)$_2$.

spectively. When these molecules interact with the Ti atom, the valence electrons of Ti overlap with the LUMO orbital. The more negative is the LUMO band energy, more likely it is for the electron to be trapped in these orbitals. Among the above molecules, O$_2$ has the lowest LUMO orbital, and as it interacts with the Ti atom, it binds strongly with the valence electron of the Ti atom. The oxygen molecule, therefore, is more reactive toward the Ti atom and is an important factor in understanding the different adsorption states.

As shown in Fig. 7(e), the Ti$_2$(Bz)$_2$ complex has a band gap of only 0.10 eV which accounts for its higher reactivity. We studied the band decomposed charge density of the HOMO band, which shows that the HOMO charge is mainly distributed around the top Ti atom which acts as a reactive site where the incoming species chemically adsorb. The NH$_3$, H$_2$, and O$_2$ molecules are found to attach to the top Ti atom in dissociative chemisorbed states and release about 2, 1, and 8 eV energies, respectively. One can see from Figs. 7(f)–7(h) that the dissociative chemisorbed states of NH$_3$, H$_2$, and O$_2$ do not alter the band gaps much. The band gaps are 0.43, 0.11, and 0.40 eV, which shows that these materials are still reactive. Thus, they could adsorb more NH$_3$, H$_2$, or O$_2$ molecules. We first checked the active adsorption site by putting a hydrogen atom on either top of the Ti atom or on the center Ti atoms of the Ti$_2$(Bz)$_2$ complex where NH$_3$, H$_2$, or O$_2$ are dissociatively adsorbed. The structures were fully relaxed. Our results show that the hydrogen atom binds stronger to the top Ti atom, which suggests that the top Ti atom is still reactive. Additional NH$_3$, H$_2$, and O$_2$ molecule were placed on the on-top Ti atom of the Ti$_2$(Bz)$_2$ complex already bound to NH$_3$, H$_2$, or O$_2$ in dissociative adsorbed state. The optimized results show that they could be adsorbed in chemisorption state. This agrees very well with the picture arrived from a band gap analysis.

IV. CONCLUSIONS

Based on our detailed first-principles calculations, we found that NH$_3$, H$_2$, and O$_2$ molecules react with Ti$_2$(Bz)$_2$ complex, but are unreactive toward Ti(Bz)$_2$ complex. On the other hand, oxygen reacts with both Ti(Bz)$_2$ and Ti$_2$(Bz)$_2$ complexes. There are no physisorption states for NH$_3$, H$_2$, and O$_2$ interacting with the exposed Ti atom of the Ti$_2$(Bz)$_2$ complex. They first bind in the molecularly chemisorbed state and the transit to the dissociative chemisorption state after overcoming a small energy barrier. The energy barriers for such transitions are about 0.43, 0.20, and 0.32 eV for NH$_3$, H$_2$, and O$_2$ adsorbed Ti$_2$(Bz)$_2$, respectively. The binding energies for the ground states of NH$_3$, H$_2$, and O$_2$ adsorbed Ti$_2$(Bz)$_2$ are 2.18, 1.14, and 8.00 eV, respectively. Only O$_2$ reacts with the Ti atom in the Ti(Bz)$_2$ complex. The reaction energy barriers for the O$_2$ transitioning from the physisorbed state to the molecularly chemisorbed state, and then to the final dissociative chemisorbed state, are about 0.06 and 0.51 eV, respectively. The final product of O$_2$ adsorbed Ti(Bz)$_2$ has a binding energy of 5.09 eV. NH$_3$ and H$_2$ prefer the physisorbed states on Ti(Bz)$_2$ complex, whose binding energies are about 0.06 and 0.11 eV, respectively. Indicated by our minimum energy path search, under special conditions such as the high pressure, one may store hydrogen in chemisorbed states on Ti(Bz)$_2$ complex. The energy barriers for transition of H$_2$ from physisorbed to the molecularly chemisorbed state, and then to the dissociative chemisorbed state, are about 0.32 and 0.45 eV, respectively. The reverse reaction to release hydrogen needs to overcome about 0.08 and 0.13 eV barriers for the transitions from the dissociative chemisorption state to the molecularly chemisorbed state and then to the physisorbed states. In Ti$_2$(Bz)$_2$ complex, the first incoming molecule would reach the dissociative chemisorption state with two isolated H atoms attached to the top Ti atom. However, the release of these hydrogen atoms needs to overcome a large barrier of about 1 eV. Upon adsorption of hydrogen around the top Ti atom, the center Ti atom can attach hydrogen in a manner similar to the center Ti atom in Ti(Bz)$_2$ complex. Therefore, under special condition, the Ti$_2$(Bz)$_2$ could also store hydrogen by adsorbing H$_2$ around the sandwiched Ti atom. The physisorption of NH$_3$ and H$_2$ on the Ti(Bz)$_2$ complex has little effect on the DOS of the metal-benzene complex due to the weak van der Waals interaction. The chemisorption of O$_2$ on Ti(Bz)$_2$ induces a large distortion of the structure, consequently changing its DOS and opening a band gap of about 2 eV. The band gaps of the NH$_3$, H$_2$, and O$_2$ adsorbed Ti$_2$(Bz)$_2$ complexes are still very small, showing their reactivity.

ACKNOWLEDGMENTS

[1] G. Wilkinson, F. G. A. Stone, and E. W. Abel, *Comprehensive Organometallic Chemistry* (Pergamon, New York, 1982).

[2] C. J. Ma and D. A. Dougherty, Chem. Rev. (Washington, D.C.) **97**, 1303 (1997).

[3] D. Braga, P. J. Dyson, F. Grepioni, and B. F. G. Johnson, Chem. Rev. (Washington, D.C.) **94**, 1585 (1994).

[4] T. Kurikawa, H. Takeda, M. Hirano, K. Judai, T. Arita, S. Nagao, A. Nakajima, and K. Kaya, Organometallics **18**, 1430 (1999).

[5] K. Hoshino, T. Kurikawa, H. Takeda, A. Nakajima, and K. Kaya, J. Phys. Chem. **99**, 3053 (1995).

[6] T. Yasuike, A. Nakajima, S. Yabushita, and K. Kaya, J. Phys. Chem. A **101**, 5360 (1997).

[7] R. Pandey, B. K. Rao, P. Jena, and M. A. Blanco, J. Am. Chem. Soc. **123**, 3799 (2001).

[8] H. Lee, W. I. Choi, and J. Ihm, Phys. Rev. Lett. **97**, 056104 (2006).

[9] S. Li and P. Jena, Phys. Rev. Lett. **97**, 209601 (2006).

[10] E. Durgun, S. Ciraci, W. Zhou, and T. Yildirim, Phys. Rev. Lett. **97**, 226102 (2006).

[11] T. Yildirim and S. Ciraci, Phys. Rev. Lett. **94**, 175501 (2005).

[12] Q. Sun, Q. Wang, P. Jena, and Y. Kawazoe, J. Am. Chem. Soc. **127**, 14582 (2005).

[13] P. Hohenberg and W. Kohn, Phys. Rev. **136**, B864 (1964).

[14] W. Kohn and L. Sham, Phys. Rev. **140**, A1133 (1965).

[15] G. Kresse and J. Hafner, Phys. Rev. B **47**, 558 (1993).

[16] G. Kresse and J. Furthmüller, Phys. Rev. B **54**, 11169 (1996).

[17] G. Kresse and D. Joubert, Phys. Rev. B **59**, 1758 (1999).

[18] P. E. Blöchl, Phys. Rev. B **50**, 17953 (1994).

[19] G. Kresse and J. Furthmüler, *The Guide of the Vienna ab-initio Simulation Package*, Austria, 2007, available for download at http://cms.mpi.univie.ac.at.vasp/.

[20] J. P. Perdew, in *Electron Structure of Solids'91*, edited by P. Ziesche and H. Eshrig (Akademie, Berlin, 1991), p. 11.

[21] J. P. Perdew and Y. Wang, Phys. Rev. B **45**, 13244 (1992).

[22] F. Rabilloud, J. Chem. Phys. **122**, 134303 (2005).

[23] A. K. Kandalam, B. K. Rao, P. Jena, and R. Pandey, J. Chem. Phys. **120**, 10414 (2004).

[24] D. R. Lide, *CRC Handbook of Chemistry and Physics 2004-2005* (CRC, Boca Raton, FL, 2005).

[25] G. Chung and M. S. Gordon, Organometallics **22**, 42 (2003).

[26] J. C. Slater, J. Chem. Phys. **41**, 3199 (1964).

[27] G. Mills, H. Jónsson, and G. K. Schenter, Surf. Sci. **324**, 305 (1995).

[28] G. Henkelman and H. Jónsson, J. Chem. Phys. **113**, 9978 (2000).

[29] G. Chen, X. G. Gong, and C. T. Chan, Phys. Rev. B **72**, 045444 (2005).

[30] S. P. Chan, G. Chen, X. G. Gong, and Z. F. Liu, Phys. Rev. Lett. **87**, 205502 (2001).

[31] L. Vaska, Acc. Chem. Res. **9**, 175 (1976).